Expression and secretion of the pro-inflammatory cytokine IL-8 is increased in colorectal cancer cells following the knockdown of non-erythroid spectrin αII

ANNE ACKERMANN, BARBARA LAFFERTON, GUIDO PLOTZ, STEFAN ZEUZEM and ANGELA BRIEGER

Medical Clinic I, Biomedical Research Laboratory, University Clinic Frankfurt, D-60590 Frankfurt am Main, Germany

Received November 12, 2019; Accepted February 25, 2020

DOI: 10.3892/ijo.2020.5026

Abstract. Non-erythroid spectrin αII (SPTAN1) expression is decreased in ~40% of cases of MLH1-deficient colorectal cancer (CRC). SPTAN1 knockdown reduces cell viability, cellular mobility and cell-cell contact formation, indicating that the SPTAN1 plays an important role in tumour growth, attachment and in regulating the tumour microenvironment. Changes in the tumour microenvironment can affect the immune response. Therefore, in the present study, proteome arrays were used to analyse the expression of 119 different chemokines and soluble receptors in CRC cell lines in which mutL homologue 1 (MLH1) or SPTAN1 were knocked down. The levels of interleukin (IL)-8 were significantly increased in the cells in which SPTAN1 was knocked down, both at the mRNA and protein level. ELISA demonstrated that the cells in which SPTAN1 was knocked down secreted increased quantities of IL-8, and chemotaxis assays revealed the enhanced trafficking of neutrophils, which was induced by media containing higher levels of IL-8. The IL-8 receptors, CRCX1 and CRCX2, were expressed in all the cell lines examined; however, their expression was not directly associated with IL-8 expression. The results of the present study thus demonstrated that CRC cells in which SPTAN1 was knocked down secreted significantly higher levels of IL-8, which in-turn increased the migration of neutrophilic granulocytes. As MLH1-deficient CRC exhibits an increased infiltration of cytotoxic T-cells and is associated with a decreased SPTAN1 expression, it can thus be hypothesized that CRC with a low SPTAN1 expression may release increased quantities of IL-8, resulting in increased immune cell infiltration.

Correspondence to: Dr Angela Brieger, Medical Clinic I, Biomedical Research Laboratory, University Clinic Frankfurt, Theodor-Stern-Kai 7, D-60590 Frankfurt am Main, Germany
E-mail: a.brieger@em.uni-frankfurt.de

Abbreviations: DAB, 3,3'-diaminobenzidine; BSA, bovine serum albumin; CRC, colorectal cancer; MMR, DNA mismatch repair; MSI, microsatellite instability; ELISA, enzyme-linked immunosorbent assay; MLH1, mutL homologue 1; MSH2, mutS homologue 2; MSH6, mutS homologue 6; SPTAN1, non-erythroid spectrin αII; PMS2, postmeiotic segregation increased 2; RFUs, relative fluorescence units

Key words: colorectal cancer, DNA mismatch repair, MLH1, SPTAN1, IL-8

Introduction

Colorectal cancer (CRC) is one of the most common types of cancer worldwide, and ~15% of all patients with CRC exhibit microsatellite instability (MSI), which is caused by a defective DNA mismatch repair (MMR) system, the origins of which can be either sporadic or hereditary. The hereditary disorder Lynch syndrome (also known as hereditary non-polyposis CRC) is the result of autosomal dominant heterozygous germline mutations in MMR genes and accounts for 2-5% of all cases of MSI-CRC (1). Germline mutations occur in one of the four key MMR genes; mutL homologue 1 (*MLH1*; chromosome 3p21.3), mutS homologue 2 (*MSH2*; chromosome 2p22-21), mutS homologue 6 (*MSH6*; chromosome 2p16) or postmeiotic segregation increased 2 (*PMS2*; chromosome 7p22.2) (2). Although patients with Lynch syndrome are predisposed to a variety of cancers, CRC is the most common type of cancer associated with Lynch syndrome (3). Sporadic cases of MSI-CRC account for ~12% of all CRC cases and have been found to be caused by hypermethylation of the MLH1 promoter. MLH1 promoter hypermethylation results in the loss of MLH1 protein expression, and is closely associated with the presence of the BRAFV600E mutation (4). In summary, MLH1 is the protein most frequently affected and relevant for MSI in CRC.

CRC with MSI is associated with improved survival rates, reduced aggressiveness and a more favourable prognosis (5,6). In a previous study by the authors, it was demonstrated that there was a close association between tumour aggressiveness and MLH1 deficiency, as well as a decreased non-erythroid spectrin αII (SPTAN1) expression (7). The decreased expression of the cytoskeletal protein, SPTAN1, was shown to be associated with decreased cell viability, cellular mobility and cell-cell contact. Furthermore, SPTAN1 expression was higher in patients with stage I CRC compared with patients with stages II-IV CRC, and the amount of SPTAN1 was lower in patients with metastatic CRC compared with patients with non-metastatic CRC (7).

One of the most important features of MSI-CRC however, is that these tumours exhibit a dense infiltration of cytotoxic

CD8-positive ($CD8^+$) T lymphocytes (8). The MSI tumour tissue infiltrating T-cells may eliminate the dysplastic precursors of tumour cells and may thus improve the survival of these cancer patients. The functionality of these T-cells appears to be fully available and functional during the early stages of tumour development (9), although it can be inactivated during tumour progression, a hallmark of cancer (10). From a therapeutic viewpoint, MSI-CRC is associated with resistance to the commonly used 5-FU chemotherapy regimen (11), whereas MSI sensitizes CRC to programmed cell death-1 immune checkpoint inhibitors (12).

Despite the fact that several groups have focused on the clinical differences between MSI-CRC and sporadic CRC, only a few proteins are currently known that may partially explain their respective characteristics. In the present study, proteome arrays were used with CRC cell lines in which MLH1 or SPTAN1 were knocked down to identify potentially relevant chemokines or receptor proteins, and to provide molecular explanations for the reduced tumour aggressiveness and increased T-cell infiltration in patients with MSI-CRC.

Materials and methods

Patients. Formalin-fixed paraffin-embedded (FFPE) tissue samples from 20 patients (who were members of a cohort of 189 patients with CRC used in a previous study) (7) were used as representative samples for the present study. Of these samples, 10 were MLH1-deficient, whereas the other 10 were MLH1-proficient with regards to expression (7). All patients included in the present study underwent bowel resection with curative intent. The characteristics of the individual tissue specimens are summarized in Table I. The expression levels of MLH1 have been previously analysed (7) and IL-8 expression was determined in the present study using immunohistochemistry for each tumour and the matching adjacent non-malignant tissue. The study was approved by the Local Ethics Committee of the University Hospital Frankfurt, all research was performed in accordance with relevant guidelines/regulations, and all patients provided written informed consent.

Cell lines and cell culture. SW620 (CCL-227), SW480 (CCL-228) and HT29 (HTB-38) CRC cell lines, as well as 293 (ATCC® CRL-1573™) cells, which are frequently used as a model of tumorigenic cells (13), were purchased from American Type Culture Collection. Colorectal HCT116 mlh1-2 cancer cells stably transfected with pcDNA3.1+/MLH1 were a gift from Professor Francoise Praz (Villejuif, France) (14).

All cells were grown in DMEM (Gibco; Thermo Fisher Scientific, Inc.) with 10% FBS (Sigma-Aldrich; Merck KGaA) and 1% penicillin-streptomycin (Sigma-Aldrich; Merck KGaA). The media for shMLH1, shSPTAN1 and pLKO.1 stably transduced cell lines additionally contained 5 μg/ml puromycin or 4 μg/ml for HCT116 mlh1-2 cells. The media for pLKO.1-neo and shSPTAN1-neo stably transduced SW620 cell lines additionally included G418 (1 mg/ml).

The cells were tested frequently for mycoplasma and characterized in June, 2018 using STR profiling, as indicated by the DSMZ online catalogue (15). STR profiling of the 8 STR loci was performed as recently described (16).

Transduction with SPTAN1 or MLH1-shRNAs. SW620, SW480, HT29, 293 and HCT116 mlh1-2 cells express SPTAN1, as well as MLH1 endogenously (17-19). To knockdown SPTAN1 or MLH1 expression in these cell lines, they were transduced with lentivirus encoding interfering MISSION® shRNA nucleic acid molecules, according to the manufacturer's protocol (MISSION® shRNA; Sigma-Aldrich; Merck KGaA). Briefly, cells were plated at a density of 3 or $5x10^5$ cells per well and transduced with 3 μg of shRNA targeting SPTAN1 (MISSION® shRNA TRCN0000053669) or 3 μg of shRNA targeting MLH1 (MISSION® shRNA TRCN0000288641) delivered through a viral vector (MISSION® pLKO.1-puro). As the control, SW620, SW480, HT29, 293 and HCT116 mlh1-2 cells were transduced with the same amount of viral vector containing non-mammalian shRNA (MISSION® pLKO.1-puro control plasmid DNA, SHC002). Transduced cells were selected for using 5 μg/ml puromycin in the cell culture medium, apart from the HCT116 mlh1-2 cells, which were selected for using 4 μg/ml puromycin.

To achieve the co-knockdown of MLH1 and SPTAN1, the SW620 cells stably transduced with pLKO.1 and shMLH1 were used for an additional lentiviral transduction using 3 μg of control shRNA (MISSION® Non-Target shRNA Control Plasmid DNA, SHC016) or shRNA targeting SPTAN1 (MISSION® shRNA TRCN0000053669) in a different lentiviral vector backbone (pLKO.1-Neo-CMV-TurboGFP™, MISSION®; Sigma-Aldrich; Merck KGaA) as described above. Transduced cells were selected for in G418 containing medium (1 mg/ml) for 8 days.

MSI testing. Single cell clones of stably transduced SW620 and SW480 cell lines were investigated for their MSI status. The cells were diluted to 10 cells/ml, and 100 μl of each was added per well to a 96-well plate and incubated for 14 days at 37˚C. After culturing the single cell clones, DNA was isolated and tested for MSI using a pentaplex PCR. A total of 5 different MSI loci; the quasimonomorphic mononucleotide repeats NR-21, BAT-26, BAT-25, NR-24 and NR-22 were amplified and subsequently fragment length analysis was performed using an ABI 3130xl Genetic Analyzer (Applied Biosystems; Thermo Fisher Scientific, Inc.) as previously described by Suraweera *et al* (20). The primer sequences used were as follows: NR-21 forward, 5'-TAAATGTATGTC TCCCCTGG-3' and reverse, 5'-FAM-ATTCCTACTCCG CATTCACA-3'; BAT-26 forward, 5'-TGACTACTTTTG ACTTCAGCC-3' and reverse, 5'-ATTO550-AACCATTCA ACATTTTTAACCC-3'; BAT-25 forward, 5'-FAM-TCG CCTCCAAGAATGTAAGT-3' and reverse, 5'-TCTGCA TTTTAACTATGGCTC-3'; NR-24 forward, 5'-CCATTG CTGAATTTTACCTC-3' and reverse, 5'-HEX-ATTGTG CCATTGCATTCCAA-3'; and NR-22 forward, 5'-GAGGCT TGTCAAGGACATAA-3' and reverse, 5'-FAM-AATTCT GATGCCATCCAGTT-3'. The interpretation of the results was based on the following features: If ≥3 of these 5 loci were detectable with somatic changes they were classified as high MSI (MSI-H); if ≤2 of the 5 markers exhibited somatic changes, they were considered low MSI (MSI-L); and if no changes were detected, they were considered microsatellite stable (MSS).

Table I. Clinicopathological characteristics of 20 patients with CRC evaluated for expression of MLH1, SPTAN1 and IL-8.

Patient	Sex	Localization relative to the splenic flexure	Age at diagnosis (years)	Year of diagnosis and surgery	Tumour	Metastases	Stage	MLH1 status	BRAF wt/BRAF V600$^{E/E2/D}$	Tumour SPTAN1 intensity compared to mucosa	IL-8 intensity in tumour tissue
2	F	Proximal	62	2014	pT2	M0	I	+		>	0
3	M	Proximal	77	2012	pT1	M0	I	+		>	n. a.
11	F	Distal	49	2014	pT1(sm3)	M0	I	+		>	+++
15	F	Distal	58	2013	pT2	M0	I	+		>	++
18	M	Distal	75	2012	pT2	M0	I	+		>	++
20	F	Proximal	65	2013	pT1(sm2)	M0	I	+		>	++
24	M	Proximal	65	2013	pT2	M0	I	+		>	+
25	M	Proximal	78	2014	pT2	M0	I	+		>	++
26	M	Proximal	72	2015	pT2	M0	I	+		>	+
27	M	Distal	76	2014	pT2	M0	I	+		>	++
164	F	Proximal	85	2016	pT1	M0	I	-	BRAF wt	<	+
170	F	Proximal	94	2014	pT4b	M0	IIC	-	BRAF V600$^{E/E2/D}$	<	n. a.
173	M	Proximal	75	2014	pT4b	M1a (LYM)	IVA	-	BRAF wt	<	++
177	M	Distal	29	2008	pT3c	M0	II	-	BRAF wt	<	+
179	M	Proximal	71	2016	pT3	M0	II	-	BRAF wt	<	+
180	M	Distal	47	2013	pT3	M1 (HEP)	IV	-	BRAF wt	<	++
183	M		46	2012	pT4b	M0	II	-	BRAF wt	<	n. a.
185	M	Proximal	41	2015	pT4b	M0	II	-	BRAF wt	=	++
186	M		64	2014	pT4b	M0	III	-	BRAF V600$^{E/E2/D}$	<	n. a.
188	F	Proximal	74	2016	pT3	M0	II	-	BRAF V600$^{E/E2/D}$	<	+++

n. a., not accessible/available; M, male; F, female; HEP, liver; LYM, distant lymph nodes; SPTAN1, non-erythroid spectrin αII; MLH1, mutL homologue 1.

Western blot analysis. Whole cell extracts (50 μg protein per lane) were isolated using CelLytic™ M (Sigma-Aldrich; Merck KGaA) with protease inhibitor cOmpleteTM (Roche), quantified using Bradford protein assay with Quick Start Bradford-Reagent (Bio-Rad Laboratories, Inc.), separated on 10% polyacrylamide gels, followed by transfer onto nitrocellulose membranes and antibody detection using standard procedures was performed as described previously (21). Membranes were blocked and antibodies were diluted in 5% non-fat dry milk in tris-buffered saline with 0.025% Tween-20 for 1 h at room temperature. The following antibodies were used: Anti-SPTAN1 (1:100, overnight shaking at 4˚C, cat. no. sc-46696; clone C-11; Santa Cruz Biotechnology, Inc.), anti-MLH1 (1:1,000, 1 h at room temperature, cat. no. 554073; clone G168-728; BD Biosciences), anti-SPTAN1 (1:1,000, overnight shaking at 4˚C, cat. no. MAB1622; EMD Millipore), anti-β-actin (1:5,000, 1 h at room temperature, cat. no. A5441; clone AC-15; Sigma-Aldrich-Merck KGaA), and for the fluorescently labelled secondary antibody, IRDye 680LT goat anti-mouse (1:20,000, 1 h at room temperature, cat. no. 926-68020, LI-COR Biosciences). Fluorescence signals were detected in the fluorescence scanner FLA-9000 Starion (Fujifilm Life Science). If indicated, the band intensity of protein expression from two western blots was quantified using Multi Gauge version 3.2 (Fujifilm, Inc.).

Proteome arrays. The Proteome Profiler Human Receptor Array, non-hematopoietic kit (cat. no. ARY012; R&D Systems) was used according to the manufacturer's protocol. This Human Soluble Receptor array allows the simultaneous detection of the relative levels of 119 different chemokines and soluble receptors, released by non-hematopoietic cells, which are spotted in a duplicate antibody pattern on nitrocellulose membranes. Protein extracts of shMLH1-, shSPTAN1- or control-shRNA stably transduced SW620 and SW480 cells were used. Briefly, proteins were extracted using lysis buffer, which was a component of this kit, supplemented with 10 μg/ml Aprotinin (Sigma-Aldrich; Merck KGaA) and 10 μg/ml leupeptin (Sigma-Aldrich; Merck KGaA). After blocking, arrayed antibody membranes were incubated with equal quantities of protein at 4˚C overnight. Subsequently, the membranes were washed 3 times in 1X wash buffer and incubated with horseradish peroxidase (HRP)-conjugated antibodies (R&D Systems) for 2 h at room temperature. After washing again, the membranes were incubated with Streptavidin-HRP (R&D Systems) for 30 min at room temperature. All antibodies and reagents (unless stated otherwise) were part of the used kit. As stated, all steps were carried out according to the manufacturer's instructions. Signals were visualized using the chemiluminescent substrate, detected using a LAS-4000 mini Luminescent Image Analyser and quantified using Multi Gauge version 3.2. The intensities of the signal spots of the target proteins were determined with subtraction of the averaged background negative control spot intensity. Data are presented as the relative expression normalized to the positive control spot intensity.

Reverse transcription-quantitative PCR (RT-qPCR). Total RNA was extracted from the cells using TRIzol reagent (Sigma-Aldrich; Merck KGaA) according to the manufacturer's protocol. First-strand cDNA was prepared from 1 μg RNA with 50 ng/μl random hexamer primers using SuperScript™ III First Strand Synthesis SuperMix (Invitrogen; Thermo Fisher Scientific, Inc.) according to the manufacturer's protocol. qPCR was performed using TaqMan® Gene Expression assays (Applied Biosystems; Thermo Fisher Scientific, Inc.) for IL-8 (Hs00174103_m1), CXCR1 (Hs00174304_m1), CXCR2 (Hs00174146_m1); GAPDH (Hs02786624_g1) was used as the housekeeping gene. qPCR reactions included 7.5 μl TaqMan Gene Expression Mastermix, 0.75 μl 2X TaqMan assay, RNase-free water and 2 μl cDNA (100 ng) in a total volume of 15 μl. The thermocycling conditions were as follows: 50˚C for 2 min, 95˚C for 10 min; followed by 50 cycles of 95˚C for 15 sec and 60˚C for 1 min, in a StepOnePlus™ Real-Time PCR system (Applied Biosystems; Thermo Fisher Scientific, Inc.). StepOne version 2.0 software was used to measure the qPCR curves. Finally, Cq values were exported and analysed in Microsoft Excel to determine the $2^{-\Delta\Delta Cq}$ values (22). All experiments were performed at least 3 times.

Enzyme-linked immunosorbent assay (ELISA). Human CRC cells were seeded at $5x10^5$ cells per well in 6-well plates. Following 48 h of incubation, the media were collected, centrifuged at 200 x g for 5 min at room temperature and stored at -20˚C until further use. The secretion of IL-8 was determined using ELISA with a Human IL-8/CXCL8 Quantikine ELISA kit (cat. no. D8000C; R&D Systems) according to the manufacturer's protocol. Duplicates of undiluted cell culture media were used for measurements and protein standard dilutions together with the negative controls were. The optical density was detected at 450 nm using an EnVision 2104 Multilabel Reader (PerkinElmer, Inc.). All experiments were performed at least 3 times.

Isolation of neutrophilic granulocytes and chemotaxis assays. Neutrophilic granulocytes were isolated from blood and collected in EDTA-tubes using polymorphprep solution (Progen Biotechnik). A total of 7.5 ml polymorphprep solution was placed into a 15 ml falcon tube, then overlayed with blood, at a ratio of 1:1 and centrifuged at 450 x g for 30 min at room temperature. The yellow plasma layer was discarded, and the neutrophilic granulocytes were placed into a fresh 15 ml falcon tube. The neutrophils were washed with PBS by centrifugation at 250 x g for 10 min at room temperature. The pellet was resuspended in 1 ml red blood cell lysis buffer (Roche Diagnostics), incubated at 37˚C for 5 min and centrifuged again at 250 x g for 5 min at room temperature. Finally, the supernatant was removed, the neutrophilic granulocytes were diluted in 1.5 ml serum-free DMEM, counted and used for the chemotaxis assay.

The chemotaxis assay was performed by seeding $5x10^5$ neutrophils in 100 μl serum-free DMEM in the upper chamber of a 24-Transwell plate. A CytoSelect™ 24-Well Chemotaxis assay 3 μm (Cell Biolabs) was used according to the manufacturer's protocol. A total of 500 μl DMEM with or without 10% FBS and 1% penicillin-streptomycin and other additives was added to the lower chambers. As a positive control DMEM with 10% FCS and penicillin-streptomycin as well as 100 ng recombinant human IL-8 (R&D Systems) was added to the

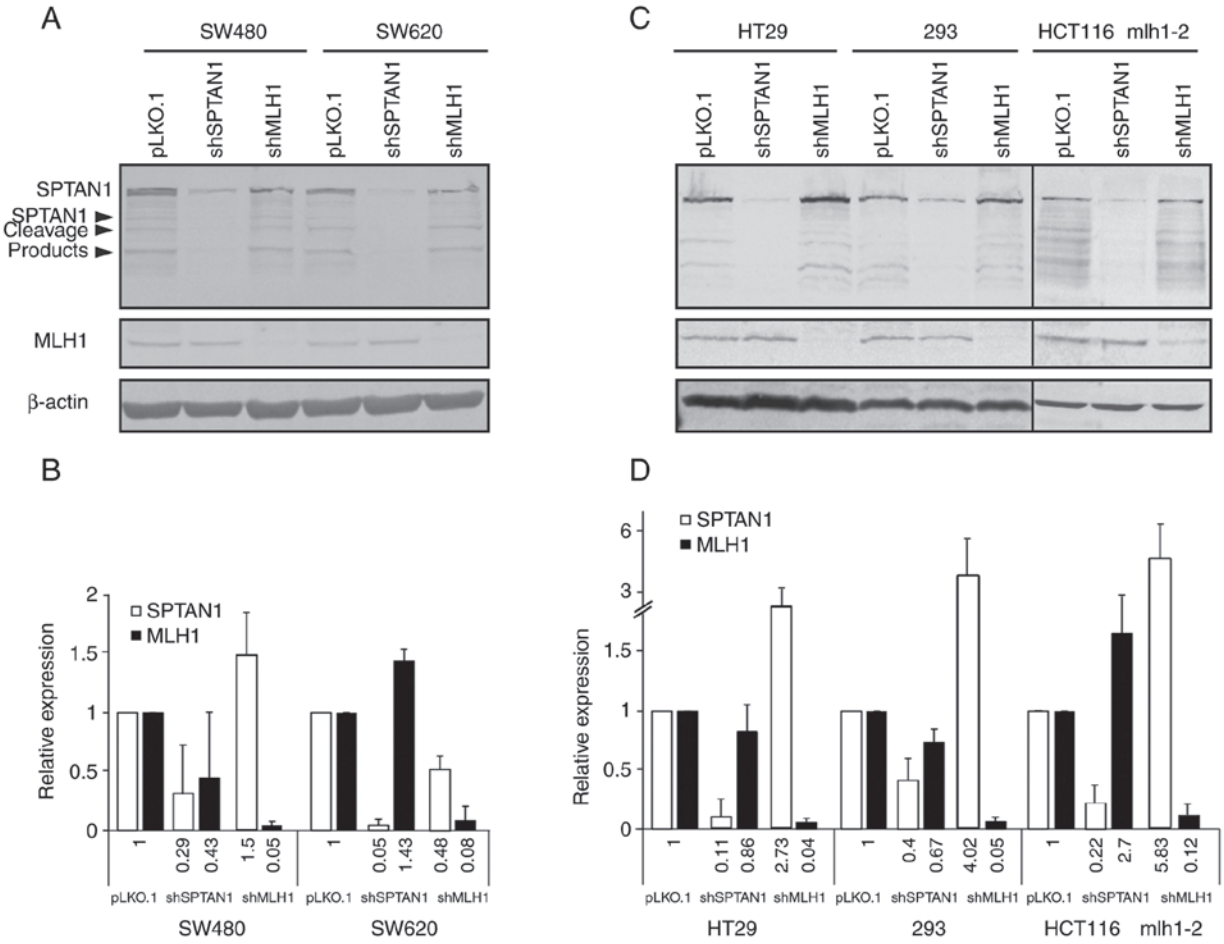

Figure 1. Stable transduction of shMLH1 and shSPTAN1. SW480, SW620, HT29, 293 and HCT116 mlh1-2 were stably transduced with shSPTAN1 and shMLH1 using lentiviral transduction. (A and C) Successful knockdown of SPTAN1 and MLH1 was verified using western blotting. (C) The western blots presented are analysed separately and cropped from different blots. The different blots are separated by black lines. The corresponding full-length western blots are presented in Fig. S3A-C. All cell lines exhibited a reduced expression of MLH1 and SPTAN1 following transduction with shMLH1 and shSPTAN1, respectively. (B and D) Densitometric analysis of the bands quantified from two western blots. Graphs show SPTAN1 (white column) or MLH1 (black column) expression normalized to the pLKO.1 transduced control cell line. Black arrows mark the cleavage products of SPTAN1. sh, short hairpin; SPTAN1, non-erythroid spectrin αII; MLH1, mutL homologue 1.

lower chamber. As a negative control, DMEM with 10% FCS and penicillin-streptomycin without further supplements was used. A total of 500 μl media obtained from SPTAN1 knockdown cells or pLKO.1 transduced control cell lines was added to the lower chamber. The 24-transwell plate was then incubated for 24 h with 5% CO_2 at 37˚C.

Subsequently, each insert was transferred to a new well and incubated with 200 μl cell detachment solution (Cell Biolabs) for 30 min at 37˚C to remove neutrophilic granulocytes adhering to the Transwell chamber. To combine migratory cells in the medium and on the bottom side of the Transwell, 400 μl of the 500 μl medium solution containing migratory cells from the lower chambers of the starting 24-Transwell plate was added. Subsequently, 180 μl of the neutrophil containing mixture was transferred into a 96-well plate, 60 μl CyQuant GR Dye solution (Cell Biolabs; diluted 1:75 in 4x lysis buffer) was added, and the samples were incubated for 20 min at room temperature. For measurements, 200 μl of each sample was transferred into a 96-well solid black microplate suitable for fluorescence measurements and measured at an excitation/emission spectra of 485/510 nm in an EnVision 2104 Multilabel Reader. The resulting data were expressed as relative fluorescence units (RFU). All experiments were performed at least 3 times.

Analysis of IL-8-251T>A polymorphism. The genotype of single nucleotide polymorphism (SNP)-251 (rs4073) (T>A) was determined in all cell lines by sequencing. Following amplification of the SNP region (forward primer, 5'-ATCCAT GATCTTGTTCTAAC-3' and reverse primer, 5'-CCCTAC TAGAGAACTTATGC-3') and generation of a 316 bp PCR product, the PCR product was purified using QIAquick PCR Purification kit (Qiagen, Inc.) and the SNP was determined by sequencing using BigDye Terminator 3.1 Ready Reaction mix (Thermo Fisher Scientific, Inc.) and DyeEx® 2.0 Spin kit (Qiagen, Inc.) on a 3130xl Genetic Analyser (Applied Biosystems; Thermo Fisher Scientific, Inc.). The human sequence of IL-8 rs4073 (NG_029889.1) was used as the reference.

Immunohistochemical analysis. IL-8 expression was analysed by immunohistochemistry using FFPE MLH1-deficient or MLH1-proficient CRC tissue, as previously described (7,18). Briefly, 2 μm sections of samples were cut from the FFPE

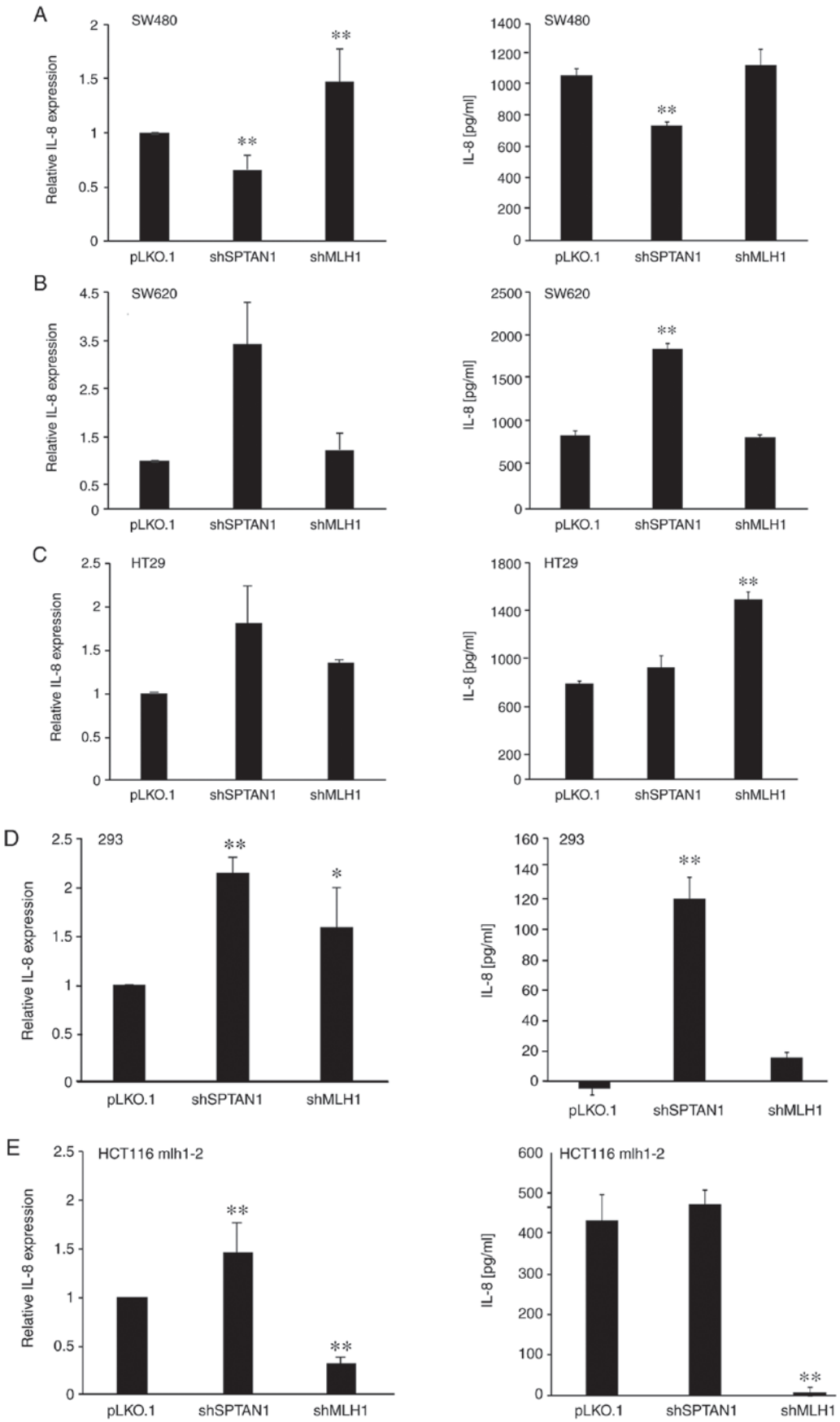

Figure 2. Relative mRNA expression and secretion of IL-8 in cells in which SPTAN1 and MLH1 were knocked down. Cells in which SPTAN1 and MLH1 were knocked down (A) SW480, (B) SW620, (C) HT29, (D) 293 and (E) HCT116 mlh1-2 were used to determine the relative mRNA expression of IL-8 (left panels), and the media from these cell lines were used to detect secreted IL-8 (right panels). Expression data are presented relative to the pLKO.1 transduced control. ELISA quantification was performed using a protein standard curve. Cells with a high IL-8 expression exhibited an increased secretion of IL-8, whereas cells with a low IL-8 expression exhibited a decreased secretion of IL-8 compared with the control cells, respectively. $^{*}P<0.05$, $^{**}P<0.01$, compared to the control. SPTAN1, non-erythroid spectrin αII; MLH1, mutL homologue 1.

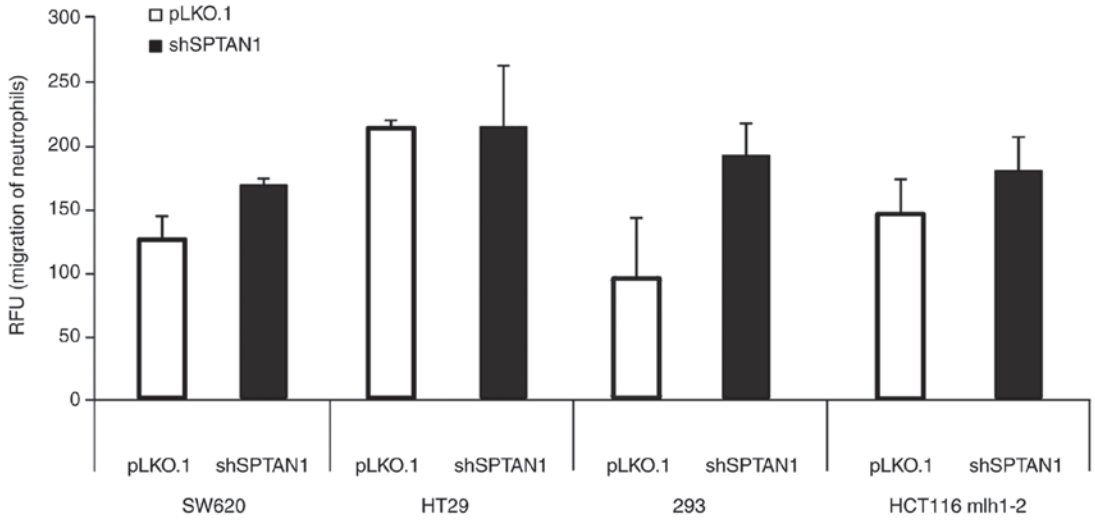

Figure 3. Induction of neutrophil migration by IL-8 secretion from cells in which SPTAN1 and MLH1 were knocked down. To analyse the effects of secreted IL-8 on the migration of neutrophilic granulocytes, chemotaxis assays were performed. Media from stably shSPTAN1 transduced cell lines were used for Transwell migration assays and neutrophil migration was determined by the fluorescence measurement of migrated cells. Media from SW620 (P=0.069), HCT116 mlh1-2 (P=0.218) and 293 cells (P=0.217) in which SPTAN1 was knocked down enhanced the migration of neutrophilic granulocytes compared with the media from pLKO.1-transduced control cells. Media from the HT29 cells in which SPTAN1 was knocked down (P=0.984) exhibited no effect on the migration of neutrophilic granulocytes compared to the media from the control cell line. RFU, relative fluorescence units; sh, short hairpin; SPTAN1, non-erythroid spectrin αII; MLH1, mutL homologue 1.

invasively growing CRC specimens. Surrounding healthy colonic mucosa served as the control. Sections were deparaffinised twice with xylene and rehydrated in a decreasing series of 5 alcohol solutions. Antigen retrieval was performed by heating in a pressure cooker for 15 min in EDTA buffer, pH 8.0. This was followed by incubation for 10 min with 3% H_2O_2 to block endogenous peroxidase activity. Sections were washed with 1X PBS (Gibco; Thermo Fisher Scientific, Inc.) before and in between incubation steps. Primary IL-8 antibody (C4; cat. no. LS-C663556; LifeSpan BioSciences, Inc.; 15 μg/ml, 1:76) was diluted in PBS containing 1% bovine serum albumin (BSA). Sections were incubated with the primary antibody at 4˚C overnight, followed by application of the EnVision System mouse (cat. no. K4000; Agilent Technologies, Inc.), which employs the enzyme HRP coupled to a secondary antibody and the chromogen 3,3'-diaminobenzidine (DAB). Samples were incubated with 4 drops of the secondary HRP-antibody for 30 min at room temperature and peroxidase reagent DAB for 10 min, diluted to 1 drop of DAB chromogen per ml of DAB substrate buffer (cat. no. K3467; Agilent Technologies, Inc.). Sections were counterstained for 2 min using Gill's haematoxylin solution (Sigma-Aldrich; Merck KGaA). Immunohistochemical staining was examined using a Keyence microscope (Model BZ-9000; Keyence Corp.). Negative controls were processed in parallel to exclude non-specific staining.

Statistical analysis. Data are expressed as the means ± standard deviation as appropriate. Data were analysed using BiAS for Windows (version 9.11) (23). RT-qPCR and chemotaxis assay data were compared using the Student's t-test or Kruskal-Wallis test for comparisons of >2 groups followed by multiple Conover-Iman post hoc tests with Bonferroni-Holm correction. Differences between IL-8 secretion measurements using ELISA were assessed for statistical significance using one-way ANOVA and post hoc Scheffe analysis. P-values are two-sided and P<0.05 was considered to indicate a statistically significant difference. Experiments were performed at least 3 times.

Results

Knockdown of SPTAN1 and MLH1 increases expression of IL-8. Using SW480 and SW620 cells stably transduced with shMLH1 or shSPTAN1 and the corresponding controls (Fig. 1A and B), the Proteome Profiler Human Soluble Receptor Array was used to analyse the cellular expression levels of 119 different chemokines and soluble receptors. The resulting mean pixel density of each spot was calculated, an averaged background signal was subtracted, and values were compared relative to the positive controls on the membrane of the human common analytes array (part C) (Fig. S1). There was a clear difference in the expression levels of the pro-inflammatory cytokine IL-8 in the cells in which SPTAN1 was knocked down in both cell lines. While the shSPTAN1-transduced SW480 cells exhibited a notable decrease in IL-8 expression (Fig. S1A and E), the shSPTAN1-transduced SW620 cells exhibited increased IL-8 expression levels (Fig. S1C and E). By contrast, the reduction of MLH1 expression in the SW480 cells resulted in an increased IL-8 expression (Fig. S1B and E), whereas MLH1 knockdown in the SW620 cells had no effect on the IL-8 levels (Fig. S1D and E).

To exclude the possibility that changes in IL-8 expression were caused by MLH1 or SPTAN1 knockdown, the induced accumulation of frameshift mutations in genes encompassing coding microsatellites, MSI was analysed in single cell clones of shMLH1- or shSPTAN1-transduced SW480 and SW620 cells. On the whole, 76 different cell clones were analysed; 12 clones of shSPTAN1-transduced SW480 cells, 14 clones of shMLH1-transduced SW480

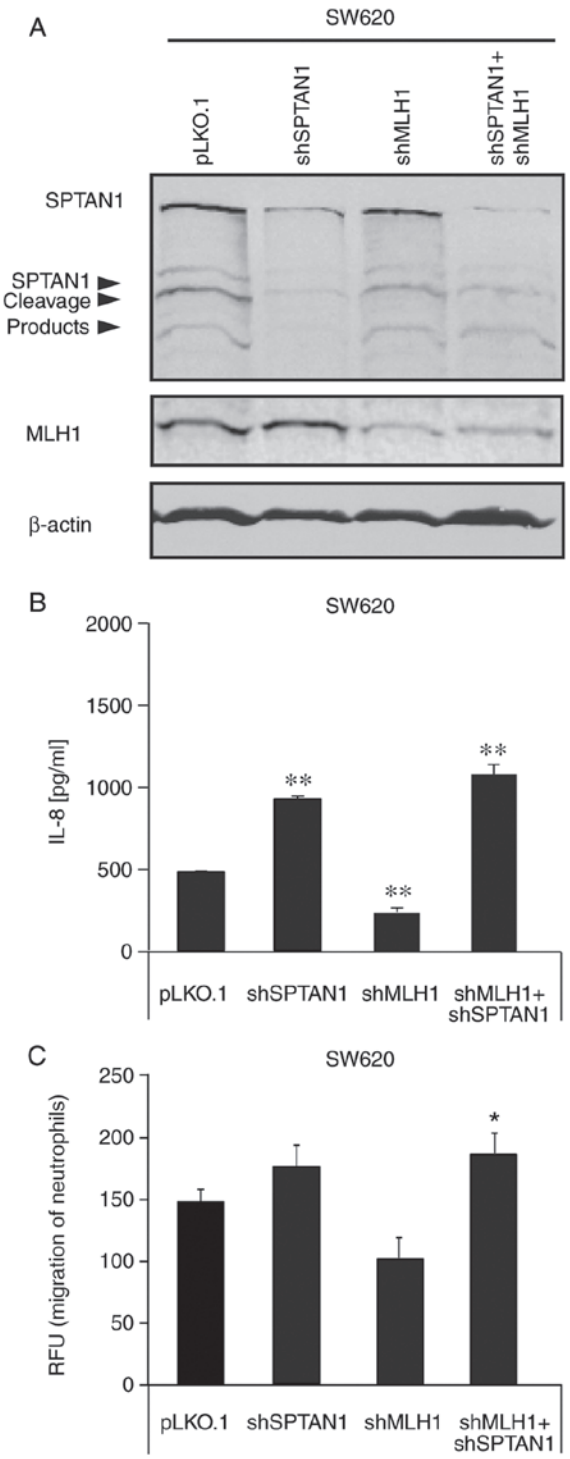

Figure 4. Loss of SPTAN1 expression underlies the increased IL-8 secretion in shSPTAN1- and shMLH1-co-transduced SW620 cells. SW620 cells transduced with shMLH1, shSPTAN1 or co-transduced with shMLH1 and shSPTAN1 were generated and (A) the success of stable transduction was confirmed using by blot analysis. The corresponding full-length western blot is shown in Fig. S3D. Media from shMLH1, SPTAN1 or co-transduced cells were used to analyse (B) IL-8 secretion and (C) effect on the migration of neutrophilic granulocytes, and the resulting data were compared with the pLKO.1-transduced controls, respectively. (B and C) IL-8 secretion in media from shMLH1-transduced SW620 cells were significantly reduced and resulted in the decreased migration of neutrophils, whereas IL-8 levels in the media from cells in which SPTAN1 was knocked down, and in media from MLH1- and SPTAN1-co-knockdown SW620 cells were significantly increased; the migration of neutrophils was also significantly increased compared with the control cells. Black arrows mark the cleavage products of SPTAN1. *P<0.05, **P<0.01, compared to the control. sh, short hairpin; SPTAN1, non-erythroid spectrin αII; MLH1, mutL homologue 1.

cells, 15 clones of pLKO.1-transduced SW480 cells, 12 clones of shSPTAN1-transduced SW620 cells, 7 clones of shMLH1-transduced SW620 cells and 16 clones of pLKO.1-transduced SW620 cells. MSI was not detected in the SW480 or SW620 cells transduced with shMLH1 or shSPTAN1 (Fig. S2 and Table SI).

Increased IL-8 mRNA expression levels are associated with a decreased SPTAN1 expression. In order to determine the effects of SPTAN1 or MLH1 knockdown on IL-8 in other cell lines, 3 additional stably-transduced shMLH1 and shSPTAN1 cell lines were generated: HT29, 293 and HCT116 mlh1-2. These cell lines (Figs. 1C and D, and S3B and C), together with the panel of SW480 and SW620 cells (Figs. 1A and B, and S3A) were used for RT-qPCR to analyse the mRNA expression levels of IL-8 (Fig. 2, left panels). The decreased expression of SPTAN1 was associated with an enhanced mRNA expression of IL-8 in 4 of the 5 tested cell lines. IL-8 was significantly enhanced in the shSPTAN1-transduced 293 (P=0.004) and HCT116 mlh1-2 cells (P=0.008), and exhibited a notable increase in the shSPTAN1-transduced SW620 (P=0.055) and HT29 (P=0.057) cells, although the increase was not considered statistically significant (Fig. 2B-E, left panels). By contrast, the knockdown of SPTAN1 significantly decreased the mRNA expression levels of IL-8 in the SW480 cells (P=0.008; Fig. 2A, left panel). The knockdown of MLH1 resulted in significantly reduced IL-8 mRNA expression levels in the HCT116 mlh1-2 (P=0.008) cells (Fig. 2E, left panel), whereas the expression of IL-8 was significantly increased in the SW480 (P=0.008) and 293 (P=0.033) cells (Fig. 2A, C and D, left panels) and also increased in the HT29 cells in which MLH1 was knocked down, although with no statistically significance (P=0.057). The knockdown of MLH1 in the SW620 cells had no marked effect on the expression of IL-8 (Fig. 2B, left panel).

Differential expression of IL-8 affects IL-8 secretion in cells in which SPTAN1 and MLH1 are knocked down. The secretion of IL-8 in the previously described knockdown cell lines was assessed using ELISA (Fig. 2, right panels) compared with the control shRNA-transfected cells. The secretion of IL-8 was associated with the mRNA expression levels of IL-8 in almost all cell lines. SW620 cells transduced with shSPTAN1 (P<0.000; Fig. 2B, right panel) and the shSPTAN1-transduced 293 cells (P<0.000; Fig. 2D, right panel) exhibited a significantly increased IL-8 secretion, whereas the shSPTAN1-transduced SW480 cells secreted significantly lower levels of IL-8 (P<0.002; Fig. 2A, right panel) compared with the control cells. The secretion of IL-8 in the shSPTAN1-transduced HT29 cells (Fig. 2C, right panel) and shSPTAN1-transduced HCT116 mlh1-2 cells (Fig. 2E, right panel) did not differ notably from that of the control cell lines, although the mRNA levels were increased (Fig. 2C and E, left panels).

HT29 cells transduced with shMLH1 (P<0.000), as well as the shMLH1-transduced 293 cells (P=0.068) exhibited an increased IL-8 secretion (Fig. 2C and D, right panels). Of note, the shMLH1-transduced HCT116 mlh1-2 cells (P<0.000) exhibited a significantly decreased secretion of IL-8 (Fig. 2E, left panel).

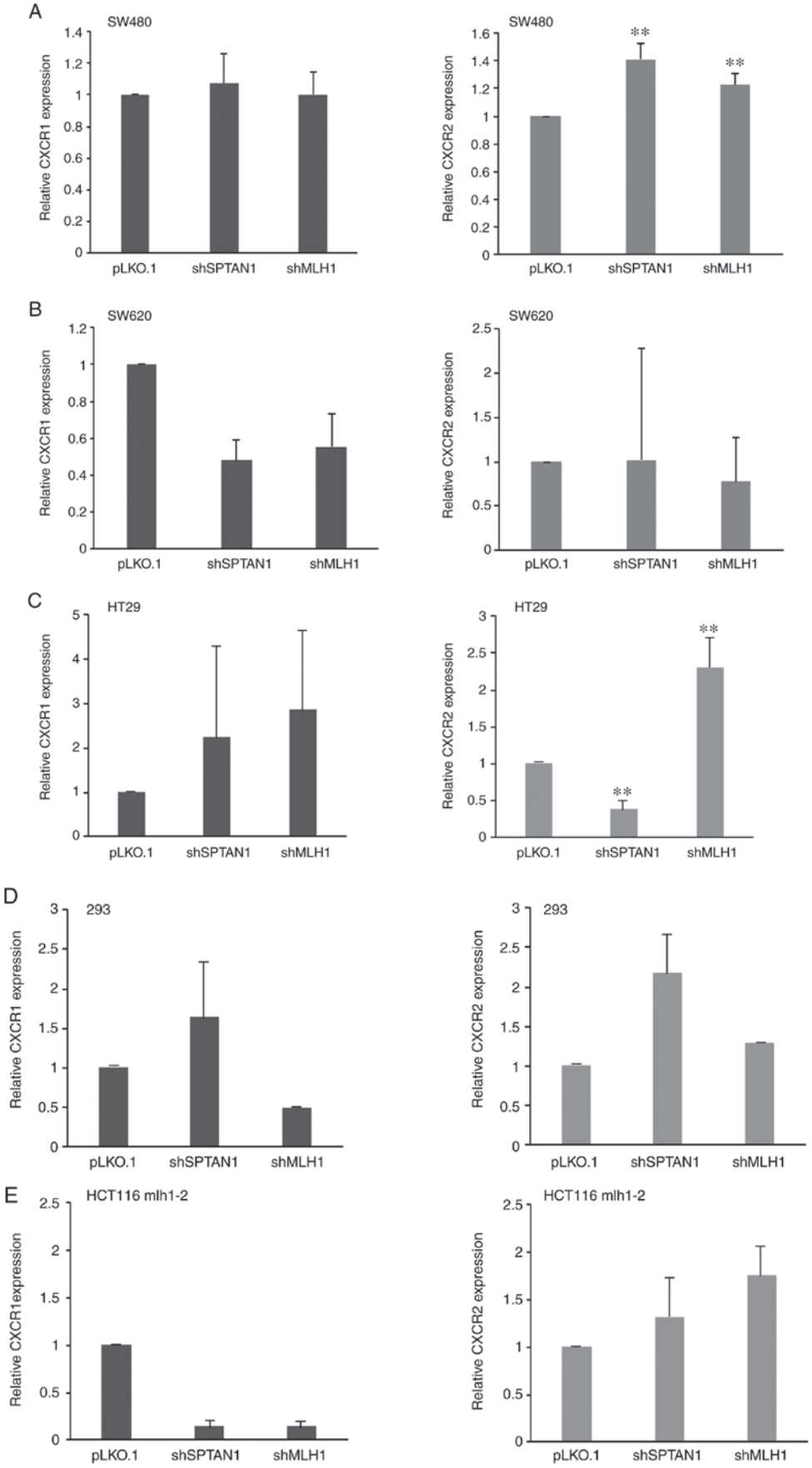

Figure 5. Relative mRNA expression of CXCR1 and CXCR2 in cells in which SPTAN1 and MLH1 were knocked down. Relative mRNA expression levels of CXCR1 (left panels) and CXCR2 (right panels) were analysed in cells in which SPTAN1 or MLH1 were knocked down. (A) SW480, (B) SW620, (C) HT29, (D) 293 and (E) HCT116 mlh1-2 cells and compared with the respective pLKO.1 transduced controls. Expression of CXCR1, as well as CXCR2 was detectable in all cell lines. However, a clear trend of receptor expression or a notable association in the expression of IL-8 could not be detected. $^{**}P<0.01$, compared to the controls. SPTAN1, non-erythroid spectrin αII; MLH1, mutL homologue 1.

Table II. IL-8-251 T/A (rs4073) SNP genotype of the analysed CRC cell lines.

Cell line	-251 T>A genotype (rs4073)
SW480	T/T
SW620	T/T
HT29	A/A
HCT116 mlh1-2	A/A
293	A/A

Induction of neutrophil migration by IL-8 using media from cell lines in which SPTAN1 was knocked down. Chemotaxis assays were performed using the media from 4 cell lines in which SPTAN1 was knocked down, the SW620, HT29, 293 and HCT116 mlh1-2 cells (Fig. 3), which all exhibited an increased secretion of IL-8 (Fig. 2). The migration of neutrophilic granulocytes was induced by the media from the shSPTAN1-transduced SW620 (P=0.069), 293 (P=0.217) and HCT116 mlh1-2 cells (P=0.218) compared with the pLKO.1-transduced controls, respectively, although the differences were not statistically significant. An induction of granulocyte migration using the media from the shSPTAN1-transduced HT29 cells (P=0.984) was not detectable (Fig. 3).

IL-8 secretion in shSPTAN1- and shMLH1-co-transduced SW620 cells is initiated by the loss of SPTAN1. To determine whether the loss of SPTAN1 expression may also result in an increased IL-8 secretion in shMLH1-transduced CRC cells, a cell line in which SPTAN1 and MLH1 were co-knocked down was generated using the SW620 cells (Fig. 4A) and compared to sister cells in which MLH1, SPTAN1 or control shRNA were used alone. As shown in Fig. 4B, the shSPTAN1-transduced (P<0.000), as well as shSPTAN1- and shMLH1-co-transduced (P<0.000) SW620 cells exhibited a significantly increased IL-8 secretion, as detected by ELISA. However, the secretion of IL-8 from the SW620 cells in which MLH1 was knocked down (P<0.000) was significantly decreased compared with that of the control cell line. In line with these data, the chemotaxis assay revealed an increased induction of the migration of neutrophilic granulocytes by media from the shSPTAN1-transduced SW620 cells (P=0.239), which was significantly increased using the media from shSPTAN1- and shMLH1-co-transduced SW620 cells (P=0.046) compared with the control (Fig. 4C). Media from the SW620 cells in which MLH1 was knocked down resulted in the decreased induction of neutrophilic granulocyte migration (P=0.254, Fig. 4C).

Expression of CXCR1 and CXCR2 is not associated with IL-8 expression. Using RT-qPCR, the expression of the corresponding IL-8 receptors, CXCR1 and CXCR2, was assessed. A consistent trend was not detected following SPTAN1 or MLH1 knockdown. In the SW480 cells, the expression of CXCR1 mRNA was not affected by the knockdown of SPTAN1 or MLH1 (Fig. 5A, left panel); however, the expression of CXCR2 was significantly increased in the shSPTAN1-transduced SW480 cells (P<0.000) and in the shMLH1-transduced SW480 cells (P=0.008, Fig. 5A, right panel). The SW620 cells transduced with shSPTAN1 and shMLH1 exhibited decreased CXCR1 mRNA levels (P=0.060, respectively; Fig. 5B, left panel); however, there was no difference in the CXCR2 mRNA levels compared with the control (Fig. 5B, right panel). The decreased expression of SPTAN1 and MLH1 resulted in the enhanced mRNA expression of CXCR1 in the HT29 cells (P=0.725, Fig. 5C, left panel), whereas CXCR2 expression was significantly decreased in the shSPTAN1-transduced cells (P=0.008) and significantly increased in the shMLH1-transduced HT29 cells (P=0.008; Fig. 5C, right panel). The mRNA expression levels of CXCR1 (P=0.202) and CXCR2 (P=0.063) were increased in the 293 cells following SPTAN1 knockdown (Fig. 5D); however, in the shMLH1-transduced 293 cells, CXCR1 expression was decreased, whereas CXCR2 expression was slightly increased (Fig. 5D). The shSPTAN1- and shMLH1-transduced HCT116 mlh1-2 cells exhibited decreased CXCR1 mRNA levels (P=0.061, Fig. 5E, left panel), whereas increased expression levels of CXCR2 were observed in the shMLH1-transduced HCT116 mlh1-2 cells (P=0.138; Fig. 5E, right panel).

Cellular IL-8 expression is not related to the IL-8 (rs4073)-251 T/A polymorphism. A SNP in the IL-8 gene (rs4073) at position-251 (T>A) has been demonstrated to be associated with inflammatory diseases and CRC (24-30). The allele A of SNP-251 (rs4073) has been shown to be associated with an increased risk of tumour development/cancer and metastasis, and a worse prognosis (25,28-31). Other studies have demonstrated that the IL-8 SNP has no effect or reduced tumour risk for the IL-8-251A genotype (24,32,33). In order to determine whether the IL-8 (rs4073)-251 T/A polymorphism was present, the DNA of all cell lines was analysed. The SW480, as well as the SW620 cells harboured the TT genotype of SNP-251 (rs4073), whereas the HT29, HCT116 mlh1-2 and 293 cells possessed the AA genotype. The results of the IL-8 SNP analysis are summarized in Table II.

Immunohistochemical analysis of IL-8. To examine IL-8 expression *in vivo*, FFPE CRC tissue from 10 patients were analysed using immunohistochemistry; exemplarily images are presented in Fig. 6. Of the samples, 10 tumours were MLH1-deficient and SPTAN1 expression was weak, and 10 were MLH1-proficient and SPTAN1 expression was strong, as previously described (7). Immunohistochemical IL-8 data were visually evaluated with regard to staining intensity and the results are summarized in Table I. IL-8 was detectable in all tested samples; however, significant differences in IL-8 expression were not observed between the MLH1-deficient and weakly SPTAN1-expressing CRC tissues, and the MLH1-proficient and strongly SPTAN1-expressing tumours. A negative control sample (without a primary antibody) of a MLH1-proficient CRC (Table I; patient 15) was processed in parallel (Fig. 6D).

Discussion

The molecular background between MSI-CRC and sporadic CRC varies significantly (34). The elucidation of the molecular factors which are associated with improved survival rates,

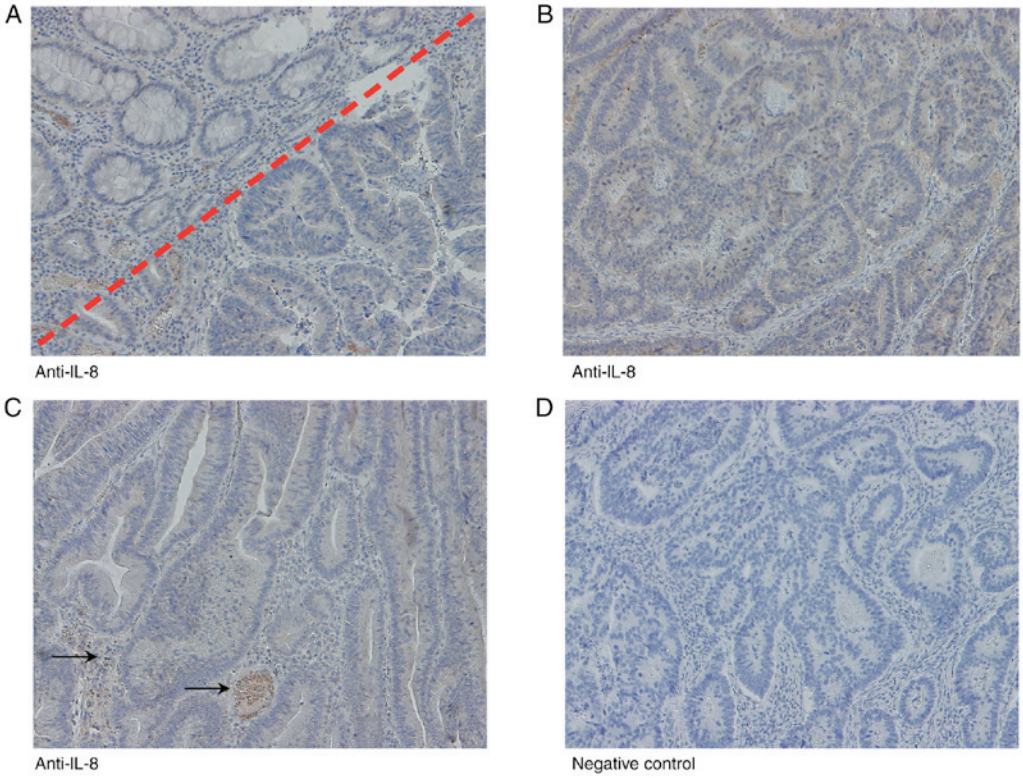

Figure 6. IL-8 protein expression in MLH1-deficient and MLH1-proficient CRC tissue samples. Immunohistochemistry images of (A) MLH1-proficient CRC (Table I, patient 18) with adjacent healthy mucosa (right lower corner), (B) a MLH1-proficient CRC (Table I, patient 15) and (C) a MLH1-deficient CRC (Table I, patient 173). (D) A negative control sample (without primary antibody) of a MLH1-proficient CRC (Table I, patient 15) was processed in parallel. Magnification, x10. (A) An MLH1-proficient CRC tissues with high SPTAN1 staining intensity exhibited increased cytoplasmic expression of IL-8 compared with the healthy mucosa. (B and C) MLH1-proficient (high SPTAN1 expressing) and MLH1-deficient (low SPTAN1 expressing) did not exhibit any significant differences in IL-8 expression. Lymphocytes and neutrophilic granulocytes in peritumoral infiltrates, as well as erythrocytes in vessels (black arrows) served as the internal positive control for IL-8 staining. CRC, colorectal cancer; SPTAN1, non-erythroid spectrin αII; MLH1, mutL homologue 1.

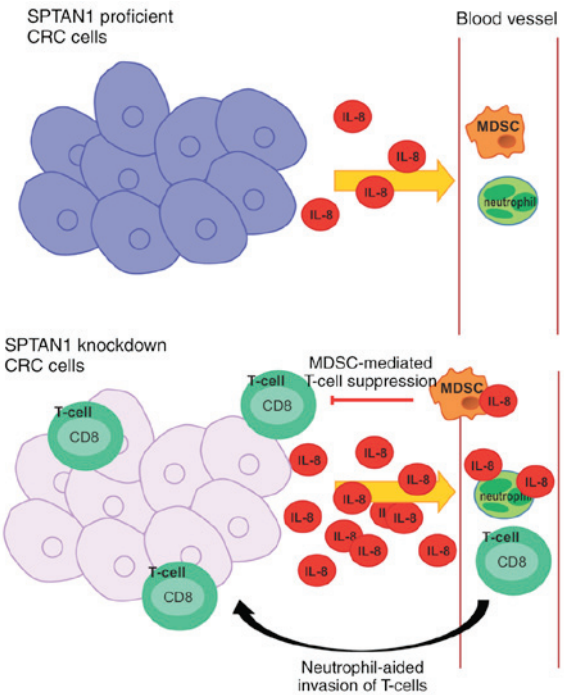

Figure 7. Hypothesis by which IL-8 induces neutrophil-mediated effects. Enhanced IL-8 production of SPTAN1-knockdown CRC cells and release in the tumor microenvironment may result in neutrophil-mediated invasion of CD8+ T-cells. In parallel, IL-8 may also attract MDSCs which mediate suppression of CD8+ T-cells. SPTAN1, non-erythroid spectrin αII; CRC, colorectal cancer; MDSC, myeloid-derived suppressor cell.

reduced aggressiveness or a more favourable prognosis of MSI-CRC are the focus of clinical research (5,6). In a previous study by the authors, it was demonstrated that ~40% of MLH1-deficient CRC cases were associated with reduced expression of SPTAN1 and reduced tumour aggressiveness (7). In the present study, the knockdown of SPTAN1 in cell lines significantly increased the levels of IL-8. Using MSI analysis, it was shown that the increase in IL-8 levels was not caused by the knockdown-dependent accumulation of frameshift mutations in genes encompassing coding microsatellites. Of the 5 cell lines transduced with shSPTAN1, 4 exhibited enhanced IL-8 mRNA levels and increased secretion of IL-8 in the media, and the media was capable of inducing migration of neutrophilic granulocytes.

IL-8, which is a member of the CXC chemokine superfamily of structurally and functionally related inflammatory cytokines, is an interesting target protein in the context of the molecular differences between MSI-CRC and sporadic CRC (34). It has been demonstrated that several types of human carcinomas, in particular CRC, express high levels of IL-8 compared with the corresponding healthy tissue (35-37). IL-8 produced by tumour cells can directly modulate neighbouring cells through its corresponding chemokine G-protein-coupled serpentine receptors, CXCR1 and CXCR2. Thuringer *et al* (38) demonstrated that the CRC line, SW620, can activate CXCR2 expressed on surrounding endothelial cells by secreting IL-8, and thus contribute to metastasis. Brew *et al* (39) demonstrated

that IL-8 acts as an autocrine growth factor on HCT116A, HCT116B and HT29 colorectal cancer cells. Furthermore, Addison *et al* (40) and Heidemann *et al* (41) demonstrated that IL-8 affects angiogenesis, and this was also mediated via CXCR2.

Additionally, secreted IL-8 is an important immune response mediator that stimulates the ability of neutrophilic granulocytes to attack injured or inflamed tissue, and chemoattractants released from these neutrophils are able to specifically attract $CD8^+$ T-cells to the site of neutrophil release (42,43). Several groups have demonstrated that the secretion of IL-8 by CRC cells results in the stimulation and migration of neutrophilic granulocytes (44,45), which mediate T-cell and monocyte accumulation (43). This has also been confirmed *in vivo* by David *et al* (46) where it was demonstrated that IL-8 and its receptors can substantially alter the infiltration of leukocytes into the tumour, which results in the accumulation of immunosuppressive and pro-tumorigenic immune cells, and results in the dysfunction of antitumor immune cells.

As demonstrated in the present study, high levels of IL-8 were associated with a decreased SPTAN1 expression, and this has previously been associated *in vivo* with MLH1-deficiency in CRC (7). As there was no clear impact of the differential secretion of IL-8 on the mRNA expression of CXCR1 and CXCR2 in the tested CRC cell lines, it was not possible to determine the effects of IL-8 on neighbouring tumour cells. However, the enhanced chemotaxis detected after using the media from shSPTAN1-transduced cells compared with the media from control cells, suggested that an enhanced IL-8 expression in colorectal tumours with a decreased SPTAN1 expression may influence the migration of neutrophilic granulocytes, which in turn may increase the invasion of the surrounding T-cells. Consistent with this hypothesis, it has been demonstrated that the enhanced infiltration of cytotoxic T-cells is associated with MMR deficiency in CRC (47,48). Therefore, an enhanced IL-8 expression and secretion may underlie increased T-cell infiltration and the reduced tumour aggressiveness of MSI-CRC (5).

During cancer or severe injury conditions, an expansion of immature and mature neutrophils has been observed to inhibit T-cell proliferation (49). These so-called myeloid-derived suppressor cells (MDSCs) can invade rapidly in tumour tissues which is induced by IL-8 (49,50). In addition, IL-8 has also been found to stimulate activated MDSCs, resulting in released DNA, and the formation of neutrophil extracellular traps (NETs) (50). NETs consist of extracellular chromatin fibers and neutrophil granular proteins adorned with antimicrobial proteins (51), and the formation of NETs in the tumour microenvironment seems to play a relevant role in the inhibition of the immune response against tumours (52-54).

Taken together, it can be hypothesized that increased IL-8 levels result in an enhanced $CD8^+$ T-cell tumour infiltration, although in parallel, it increases activation of MDSCs which may result in the cancelling of each other's effects (Fig. 7). The observation of an enhanced infiltration of cytotoxic T-cells in MMR deficient CRC fits this hypothesis (47,48).

Of note, the increased expression of IL-2 and TNF-α has recently been demonstrated to be associated with low levels of expression of MLH1, MSH2 and MSH6 in CRC (55). Although it was postulated that the detected IL-2 and TNF-α levels may be regulated by T-cells, the results of the present and previous studies (56) demonstrated that cancer cells are able to actively secrete chemokines. Therefore, the detected expression of high IL-2 and TNF-α levels shown in the study by Germini *et al* (55) may also be the result of the tumour cells themselves.

The question remains why the effect of MLH1 knockdown on IL-8 varied and why these results were not completely consistent with those generated by shSPTAN1-transduced cells, even though there was an association between MLH1-deficiency and SPTAN1 expression in CRC (7,18). The loss of MLH1 was associated with enhanced IL-8 levels in only 2 of the 5 cell lines, whereas two other cell lines exhibited a decrease in IL-8 levels and one cell line did not exhibit any notable changes. It may be possible that the SNP in IL-8 at position-251 (T>A) (rs4073) affects the expression levels of IL-8 in the present study. However, the influence of the IL-8 polymorphisms at position-251 could be excluded, since two different CRC cell lines from the same patient [SW480 (from the primary tumour) and SW620 cells (from the metastasis)], which harbour the same IL-8 SNP [-251 TT (rs4073)], exhibited differential effects with regards to IL-8 expression following SPTAN1 or MLH1 knockdown. Therefore, it may be the case that the time period allowed for shMLH1 transduction was not sufficient to induce the reduction in SPTAN1 expression in all of the cell lines and to thus increase IL-8 secretion. The results of the present study demonstrated that cells in which MLH1 and SPTAN1 were co-knocked down (exemplarily demonstrated with the SW620 cells) exhibited an increased secretion of IL-8 and an enhanced induction of neutrophil migration compared to the cells transduced only with shMLH1. MLH1 knockdown alone was not sufficient to enhance the quantity of IL-8 secreted in this cell line, whereas SPTAN1 knockdown was sufficient.

Finally, the analysis of IL-8 expression was investigated *in vivo* using a small panel of CRC tissues, consisting of 10 MLH1-deficient and 10 MLH1-proficient CRC tissues. The intensity of IL-8 in the analysed tissues was low, whereas the general detection of IL-8 was successful, as the IL-8 of erythrocytes (used as a positive control) was detectable (57). Overall, there were no significant differences in IL-8 levels detected between MLH1-deficient and MLH1-proficient tumours. However, it is necessary to verify these results using a larger study cohort. Thus, the effect of IL-8 on tumour progression of MLH1-deficient tumours and sporadic CRC should not be excluded.

In conclusion, the present study demonstrated that SPTAN1 knockdown in CRC cells significantly increased IL-8 levels and induced the migration of neutrophil granulocytes. Further studies are required to determine whether IL-8 secreted by CRC cells in which SPTAN1 is knocked down can also induce the formation of NETs and to determine the underlying signalling pathways, as IL-8 may serve as a suitable target for personalized therapy of patients with CRC.

Acknowledgements

The authors would like to thank Dr Ria Winkelmann (Dr. Senckenberg Institute of Pathology, University Hospital Frankfurt, Frankfurt am Main, Germany) for the classification

of the tissues. The results shown in this manuscript are in part data of the PhD thesis of Anne Ackermann.

Funding

The present study was supported by the Wilhelm Sander Foundation (grant no. 2014.169.1), Paul und Ursula Klein-Stiftung and institutional funds of the University Clinic Frankfurt. The funders provided salaries for research staff or consumables and had no role in design of the study, data collection and analysis, decision to publish, or preparation of the manuscript.

Availability of data and materials

All data generated or analysed during this study are included in this published article.

Authors' contributions

AA and AB were responsible for the collection and interpretation of the data. AA, AB, GP and SZ were responsible for the conception and design of the study. AA performed the majority of the experiments and analysed the data. BL performed reverse transcription-quantitative PCR and ELISA in part, and the chemotaxis assays. AA, GP and SZ critically revised and edited the manuscript. AB wrote the manuscript.

Ethics approval and consent to participate

The study was approved by the Local Ethics Committee of the University Hospital Frankfurt, all research was performed in accordance with relevant guidelines/regulations, and all patients provided written informed consent.

Patient consent for publication

Not applicable.

Competing interests

The authors declare that they have no competing interests.

References

1. Lynch HT, Snyder CL, Shaw TG, Heinen CD and Hitchins MP: Milestones of Lynch syndrome: 1895-2015. Nat Rev Cancer 15: 181-194, 2015.
2. Peltomäki P: Lynch syndrome genes. Fam Cancer 4: 227-232, 2005.
3. Bonadona V, Bonaïti B, Olschwang S, Grandjouan S, Huiart L, Longy M, Guimbaud R, Buecher B, Bignon YJ, Caron O, *et al*: Cancer risks associated with germline mutations in MLH1, MSH2, and MSH6 genes in Lynch syndrome. JAMA 305: 2304-2310, 2011.
4. Deng G, Bell I, Crawley S, Gum J, Terdiman JP, Allen BA, Truta B, Sleisenger MH and Kim YS: BRAF mutation is frequently present in sporadic colorectal cancer with methylated hMLH1, but not in hereditary nonpolyposis colorectal cancer. Clin Cancer Res 10: 191-195, 2004.
5. Gryfe R, Kim H, Hsieh ET, Aronson MD, Holowaty EJ, Bull SB, Redston M and Gallinger S: Tumor microsatellite instability and clinical outcome in young patients with colorectal cancer. N Engl J Med 342: 69-77, 2000.
6. Jeong SY, Shin KH, Shin JH, Ku JL, Shin YK, Park SY, Kim WH and Park JG: Microsatellite instability and mutations in DNA mismatch repair genes in sporadic colorectal cancers. Dis Colon Rectum 46: 1069-1077, 2003.
7. Ackermann A, Schrecker C, Bon D, Friedrichs N, Bankov K, Wild P, Plotz G, Zeuzem S, Herrmann E, Hansmann ML and Brieger A: Downregulation of SPTAN1 is related to MLH1 deficiency and metastasis in colorectal cancer. PLoS One 14: e0213411, 2019.
8. Michel S, Benner A, Tariverdian M, Wentzensen N, Hoefler P, Pommerencke T, Grabe N, von Knebel Doeberitz M and Kloor M: High density of FOXP3-positive T cells infiltrating colorectal cancers with microsatellite instability. Br J Cancer 99: 1867-1873, 2008.
9. Kloor M, Huth C, Voigt AY, Benner A, Schirmacher P, von Knebel Doeberitz M and Bläker H: Prevalence of mismatch repair-deficient crypt foci in Lynch syndrome: A pathological study. Lancet Oncol 13: 598-606, 2012.
10. Kelderman S, Schumacher TN and Haanen JB: Acquired and intrinsic resistance in cancer immunotherapy. Mol Oncol 8: 1132-1139, 2014.
11. Ribic CM, Sargent DJ, Moore MJ, Thibodeau SN, French AJ, Goldberg RM, Hamilton SR, Laurent-Puig P, Gryfe R, Shepherd LE, *et al*: Tumor microsatellite-instability status as a predictor of benefit from fluorouracil-based adjuvant chemotherapy for colon cancer. N Engl J Med 349: 247-257, 2003.
12. Mandal R, Samstein RM, Lee KW, Havel JJ, Wang H, Krishna C, Sabio EY, Makarov V, Kuo F, Blecua P, *et al*: Genetic diversity of tumors with mismatch repair deficiency influences anti-PD-1 immunotherapy response. Science 364: 485-491, 2019.
13. Stepanenko AA and Dmitrenko VV: HEK293 in cell biology and cancer research: Phenotype, karyotype, tumorigenicity, and stress-induced genome-phenotype evolution. Gene 569: 182-190, 2015.
14. Jacob S, Aguado M, Fallik D and Praz F: The role of the DNA mismatch repair system in the cytotoxicity of the topoisomerase inhibitors camptothecin and etoposide to human colorectal cancer cells. Cancer Res 61: 6555-6562, 2001.
15. DSMZ: Catalogue of human and animal cell lines, 2012.
16. Dirks WG, Faehnrich S, Estella IA and Drexler HG: Short tandem repeat DNA typing provides an international reference standard for authentication of human cell lines. ALTEX 22: 103-109, 2005.
17. Hinrichsen I, Ackermann A, Düding T, Graband A, Filmann N, Plotz G, Zeuzem S and Brieger A: Loss of MLH1 sensitizes colon cancer cells to DNA-PKcs inhibitor KU60648. Mol Carcinog 56: 1816-1824, 2017.
18. Hinrichsen I, Ernst BP, Nuber F, Passmann S, Schäfer D, Steinke V, Friedrichs N, Plotz G, Zeuzem S and Brieger A: Reduced migration of MLH1 deficient colon cancer cells depends on SPTAN1. Mol Cancer 13: 11, 2014.
19. Peng W, Tan S, Xu Y, Wang L, Qiu D, Cheng C, Lin Y, Liu C, Li Z, Li Y, *et al*: LC-MS/MS metabolome analysis detects the changes in the lipid metabolic profiles of dMMR and pMMR cells. Oncol Rep 40: 1026-1034, 2018.
20. Suraweera N, Duval A, Reperant M, Vaury C, Furlan D, Leroy K, Seruca R, Iacopetta B and Hamelin R: Evaluation of tumor microsatellite instability using five quasimonomorphic mononucleotide repeats and pentaplex PCR. Gastroenterology 123: 1804-1811, 2002.
21. Brieger A, Plotz G, Zeuzem S and Trojan J: Thymosin beta 4 expression and nuclear transport are regulated by hMLH1. Biochem Biophys Res Commun 364: 731-736, 2007.
22. Livak KJ and Schmittgen TD: Analysis of relative gene expression data using real-time quantitative PCR and the 2(-Delta Delta C(T)) method. Methods 25: 402-408, 2001.
23. Ackermann H: Bias-a program package for biometrical analysis of samples. Computational Statistics Data Analysis 11: 223-224, 1991.
24. Landi S, Moreno V, Gioia-Patricola L, Guino E, Navarro M, de Oca J, Capella G and Canzian F; Bellvitge Colorectal Cancer Study Group: Association of common polymorphisms in inflammatory genes interleukin (IL)6, IL8, tumor necrosis factor alpha, NFKB1, and peroxisome proliferator-activated receptor gamma with colorectal cancer. Cancer Res 63: 3560-3566, 2003.
25. Gunter MJ, Canzian F, Landi S, Chanock SJ, Sinha R and Rothman N: Inflammation-related gene polymorphisms and colorectal adenoma. Cancer Epidemiol Biomarkers Prev 15: 1126-1131, 2006.

26. Mustapha MA, Shahpudin SN, Aziz AA and Ankathil R: Risk modification of colorectal cancer susceptibility by interleukin-8-251T>A polymorphism in Malaysians. World J Gastroenterol 18: 2668-2673, 2012.
27. Walczak A, Przybylowska K, Dziki L, Sygut A, Chojnacki C, Chojnacki J, Dziki A and Majsterek I: The IL-8 and IL-13 gene polymorphisms in inflammatory bowel disease and colorectal cancer. DNA Cell Biol 31: 1431-1438, 2012.
28. Bondurant KL, Lundgreen A, Herrick JS, Kadlubar S, Wolff RK and Slattery ML: Interleukin genes and associations with colon and rectal cancer risk and overall survival. Int J Cancer 132: 905-915, 2013.
29. Wang N, Zhou R, Wang C, Guo X, Chen Z, Yang S and Li Y: -251 T/A polymorphism of the interleukin-8 gene and cancer risk: A HuGE review and meta-analysis based on 42 case-control studies. Mol Biol Rep 39: 2831-2841, 2012.
30. Gonzalez-Hormazabal P, Romero S, Musleh M, Bustamante M, Stambuk J, Pisano R, Lanzarini E, Chiong H, Rojas J, Castro VG, *et al*: IL-8-251T>A (rs4073) polymorphism is associated with prognosis in gastric cancer patients. Anticancer Res 38: 5703-5708, 2018.
31. Lurje G, Zhang W, Schultheis AM, Yang D, Groshen S, Hendifar AE, Husain H, Gordon MA, Nagashima F, Chang HM and Lenz HJ: Polymorphisms in VEGF and IL-8 predict tumor recurrence in stage III colon cancer. Ann Oncol 19: 1734-1741, 2008.
32. Cacev T, Radosevic S, Krizanac S and Kapitanović S: Influence of interleukin-8 and interleukin-10 on sporadic colon cancer development and progression. Carcinogenesis 29: 1572-1580, 2008.
33. Wilkening S, Tavelin B, Canzian F, Enquist K, Palmqvist R, Altieri A, Hallmans G, Hemminki K, Lenner P and Försti A: Interleukin promoter polymorphisms and prognosis in colorectal cancer. Carcinogenesis 29: 1202-1206, 2008.
34. Ali H, Bitar MS, Al Madhoun A, Marafie M and Al-Mulla F: Functionally-focused algorithmic analysis of high resolution microarray-CGH genomic landscapes demonstrates comparable genomic copy number aberrations in MSI and MSS sporadic colorectal cancer. PLoS One 12: e0171690, 2017.
35. Lee YS, Choi I, Ning Y, Kim NY, Khatchadourian V, Yang D, Chung HK, Choi D, LaBonte MJ, Ladner RD, *et al*: Interleukin-8 and its receptor CXCR2 in the tumour microenvironment promote colon cancer growth, progression and metastasis. Br J Cancer 106: 1833-1841, 2012.
36. McClelland MR, Carskadon SL, Zhao L, White ES, Beer DG, Orringer MB, Pickens A, Chang AC and Arenberg DA: Diversity of the angiogenic phenotype in non-small cell lung cancer. Am J Respir Cell Mol Biol 36: 343-350, 2007.
37. Waugh DJ and Wilson C: The interleukin-8 pathway in cancer. Clin Cancer Res 14: 6735-6741, 2008.
38. Thuringer D, Berthenet K, Cronier L, Solary E and Garrido C: Primary tumor- and metastasis-derived colon cancer cells differently modulate connexin expression and function in human capillary endothelial cells. Oncotarget 6: 28800-28815, 2015.
39. Brew R, Erikson JS, West DC, Kinsella AR, Slavin J and Christmas SE: Interleukin-8 as an autocrine growth factor for human colon carcinoma cells in vitro. Cytokine 12: 78-85, 2000.
40. Addison CL, Daniel TO, Burdick MD, Liu H, Ehlert JE, Xue YY, Buechi L, Walz A, Richmond A and Strieter RM: The CXC chemokine receptor 2, CXCR2, is the putative receptor for ELR+ CXC chemokine-induced angiogenic activity. J Immunol 165: 5269-5277, 2000.
41. Heidemann J, Ogawa H, Dwinell MB, Rafiee P, Maaser C, Gockel HR, Otterson MF, Ota DM, Lugering N, Domschke W and Binion DG: Angiogenic effects of interleukin 8 (CXCL8) in human intestinal microvascular endothelial cells are mediated by CXCR2. J Biol Chem 278: 8508-8515, 2003.
42. Hess C, Means TK, Autissier P, Woodberry T, Altfeld M, Addo MM, Frahm N, Brander C, Walker BD and Luster AD: IL-8 responsiveness defines a subset of CD8 T cells poised to kill. Blood 104: 3463-3471, 2004.
43. Taub DD, Anver M, Oppenheim JJ, Longo DL and Murphy WJ: T lymphocyte recruitment by interleukin-8 (IL-8). IL-8-induced degranulation of neutrophils releases potent chemoattractants for human T lymphocytes both in vitro and in vivo. J Clin Invest 97: 1931-1941, 1996.
44. Kelly CP, Keates S, Siegenberg D, Linevsky JK, Pothoulakis C and Brady HR: IL-8 secretion and neutrophil activation by HT-29 colonic epithelial cells. Am J Physiol 267: G991-G997, 1994.
45. Godaly G, Hang L, Frendèus B and Svanborg C: Transepithelial neutrophil migration is CXCR1 dependent in vitro and is defective in IL-8 receptor knockout mice. J Immunol 165: 5287-5294, 2000.
46. David JM, Dominguez C, Hamilton DH and Palena C: The IL-8/IL-8R Axis: A double agent in tumor immune resistance. Vaccines (Basel) 4: pii: E22, 2016.
47. Buckowitz A, Knaebel HP, Benner A, Bläker H, Gebert J, Kienle P, von Knebel Doeberitz M and Kloor M: Microsatellite instability in colorectal cancer is associated with local lymphocyte infiltration and low frequency of distant metastases. Br J Cancer 92: 1746-1753, 2005.
48. Kloor M and von Knebel Doeberitz M: The immune biology of microsatellite-unstable cancer. Trends Cancer 2: 121-133, 2016.
49. Aarts CEM and Kuijpers TW: Neutrophils as myeloid-derived suppressor cells. Eur J Clin Invest 48 (Suppl 2): e12989, 2018.
50. Alfaro C, Teijeira A, Oñate C, Pérez G, Sanmamed MF, Andueza MP, Alignani D, Labiano S, Azpilikueta A, Rodriguez-Paulete A, *et al*: Tumor-produced Interleukin-8 attracts human myeloid-derived suppressor cells and elicits extrusion of neutrophil extracellular traps (NETs). Clin Cancer Res 22: 3924-3936, 2016.
51. Brinkmann V, Reichard U, Goosmann C, Fauler B, Uhlemann Y, Weiss DS, Weinrauch Y and Zychlinsky A: Neutrophil extracellular traps kill bacteria. Science 303: 1532-1535, 2004.
52. Gonzalez-Aparicio M and Alfaro C: Influence of Interleukin-8 and Neutrophil Extracellular Trap (NET) formation in the tumor microenvironment: Is there a pathogenic role? J Immunol Res 2019: 6252138, 2019.
53. Najmeh S, Cools-Lartigue J, Rayes RF, Gowing S, Vourtzoumis P, Bourdeau F, Giannias B, Berube J, Rousseau S, Ferri LE and Spicer JD: Neutrophil extracellular traps sequester circulating tumor cells via β1-integrin mediated interactions. Int J Cancer 140: 2321-2330, 2017.
54. Alfaro C, Sanmamed MF, Rodriguez-Ruiz ME, Teijeira Á, Oñate C, González Á, Ponz M, Schalper KA, Pérez-Gracia JL and Melero I: Interleukin-8 in cancer pathogenesis, treatment and follow-up. Cancer Treat Rev 60: 24-31, 2017.
55. Germini DE, Franco MIF, Fonseca FLA, de Sousa Gehrke F, da Costa Aguiar Alves Reis B, Cardili L, Oshima CTF, Theodoro TR and Waisberg J: Association of expression of inflammatory response genes and DNA repair genes in colorectal carcinoma. Tumour Biol 42: 1010428319843042, 2019.
56. Setrerrahmane S and Xu H: Tumor-related interleukins: Old validated targets for new anti-cancer drug development. Mol Cancer 16: 153, 2017.
57. Darbonne WC, Rice GC, Mohler MA, Apple T, Hébert CA, Valente AJ and Baker JB: Red blood cells are a sink for interleukin 8, a leukocyte chemotaxin. J Clin Invest 88: 1362-1369, 1991.